Change in terrestrial ecosystem water-use efficiency over the last three decades

Authors: Mengtian Huang, Shilong Piao, Yan Sun, Philippe Ciais, Lei Cheng, Jiafu Mao, & Ben Poulter

Huang, Mengtian, Shilong Piao, Yan Sun, Philippe Ciais, Lei Cheng, Jiafu Mao, and Ben Poulter. "Change in terrestrial ecosystem water-use efficiency over the last three decades." Global Change Biology 21, no. 6: 2366-2378. DOI: https://dx.doi.org/10.1111/gcb.12873.

Change in terrestrial ecosystem water-use efficiency over the last three decades

Mengtian Huang[1], Shilong Piao[1,2], Yan Sun[1], Philippe Ciais[3], Lei Cheng[4], Jiafu Mao[5], Ben Poulter[6], Xiaoying Shi[5], Zhenzhong Zeng[1], and Yingping Wang[7]

[1]Sino-French Institute for Earth System Science, College of Urban and Environmental Sciences, Peking University, Beijing 100871, China, [2]Key Laboratory of Alpine Ecology and Biodiversity, Institute of Tibetan Plateau Research, Center for Excellence in Tibetan Earth Science, Chinese Academy of Sciences, Beijing 100085, China, [3]LSCE, UMR CEA-CNRS, Bat. 709, CE, L'Orme des Merisiers, F-91191 Gif-sur-Yvette, France, [4]CSIRO Land and Water Flagship, GPO Box 1666, Canberra ACT 2601, Australia, [5]Climate Change Science Institute and Environmental Sciences Division, Oak Ridge National Laboratory, 1 Bethel Valley Road, Oak Ridge, TN 37831-6301, USA, [6]Institute on Ecosystems and the Department of Ecology, Montana State University, Bozeman, MT 59717, USA, [7]CSIRO Ocean and Atmosphere Flagship, PMB 1, Aspendale, Vic. 3195, Australia

Abstract

Defined as the ratio between gross primary productivity (GPP) and evapotranspiration (ET), ecosystem-scale water-use efficiency (EWUE) is an indicator of the adjustment of vegetation photosynthesis to water loss. The processes controlling EWUE are complex and reflect both a slow evolution of plants and plant communities as well as fast adjustments of ecosystem functioning to changes of limiting resources. In this study, we investigated EWUE trends from 1982 to 2008 using data-driven models derived from satellite observations and process-oriented carbon cycle models. Our findings suggest positive EWUE trends of 0.0056, 0.0007 and 0.0001 g C m^{-2} mm^{-1} yr^{-1} under the single effect of rising CO_2 ('CO_2'), climate change ('CLIM') and nitrogen deposition ('NDEP'), respectively. Global patterns of EWUE trends under different scenarios suggest that (i) EWUE-CO_2 shows global increases, (ii) EWUE-CLIM increases in mainly high latitudes and decreases at middle and low latitudes, (iii) EWUE-NDEP displays slight increasing trends except in west Siberia, eastern Europe, parts of North America and central Amazonia. The data-driven MTE model, however, shows a slight decline of EWUE during the same period (−0.0005 g C m^{-2} mm^{-1} yr^{-1}), which differs from process-model (0.0064 g C m^{-2} mm^{-1} yr^{-1}) simulations with all drivers taken into account. We attribute this discrepancy to the fact that the nonmodeled physiological effects of elevated CO_2 reducing stomatal conductance and transpiration (TR) in the MTE model. Partial correlation analysis between EWUE and climate drivers shows similar responses to climatic variables with the data-driven model and the process-oriented models across different ecosystems. Change in water-use efficiency defined from transpiration-based WUE_t (GPP/TR) and inherent water-use efficiency ($IWUE_t$, GPP×VPD/TR) in response to rising CO_2, climate change, and nitrogen deposition are also discussed. Our analyses will facilitate mechanistic understanding of the carbon–water interactions over terrestrial ecosystems under global change.

Introduction

Ecosystem water-use efficiency (EWUE) is defined here as the ratio between annual gross primary productivity (GPP) and annual evapotranspiration (ET). It indicates the coupling of the carbon and water gross fluxes exchanged between ecosystem and the atmosphere, and monitors the adaptability of an ecosystem to vari-able climate conditions (Tian et al., 2010; Pe~nuelas et al., 2011; Ito & Inatomi, 2012; Keenan et al., 2013). Globally, averaged atmospheric CO_2 concentration has increased at a mean annual rate of 1.7 ppm yr1 over the past three decades (IPCC, 2013), but the resultant warming has been variable, and precipitation has increased or has decreased in different regions. These changes will likely alter the ecological functioning of terrestrial ecosys-tems, as well as the structure of plant communities. More specifically, changes in ecosystem structure, for example, the shift toward recruitment of more drought-tolerant species in regions with decreasing precipitation (Delucia & Heckathorn, 1989; Lasch et al., 2002), changes in physiological processes, such as stomatal control (Beer et al., 2009) or canopy leaf area (Kergoat et al., 2002), and changes in biogeochemical processes, such as increased carbon allocation to roots in response to decreased precipitation (Litton *et al.*, 2007; Chapin *et al.*, 2011), can all individually or interactively modify EWUE. Thus, a deeper understanding of how EWUE has responded to past climate change and increased CO_2 concentration will provide insight into how carbon and water cycles will change under future CO_2 and climate conditions (Niu *et al.*, 2011; Zhu *et al.*, 2011).

Confronted by global change, a series of ecosystem responses occurs from leaf to plant and ecosystem level, which affect ecosystem function and structure. For example, elevated CO_2 effect should enhance leaf-level 'intrinsic' WUE (WUE_i, defined as the carbon assimilation rate (A) divided by stomatal conductance (g_s)), by improving A and (or) reducing g_s (Morison, 1985). Multiyear free-air CO_2 enrichment (FACE) experiments with elevated CO_2 confirmed this theory with elevated CO_2 concentration (567 μmol mol^{-1}) decreasing g_s by over 30% and enhancing light-saturated CO_2 uptake by ~30% for C3 grass (Ainsworth & Rogers, 2007). Previous real-world ecosystem-scale studies used the metric of inherent water-use efficiency (IWUE, defined as the product of vapor pressure deficit and EWUE), and their results also suggested positive responses of IWUE to increasing ambient atmospheric CO_2 for both forest (Gagen *et al.*, 2011; De Kauwe *et al.*, 2013; Keenan *et al.*, 2013) and grassland ecosystems (Ainsworth & Rogers, 2007) over the past several decades. Using long-term eddy-covariance flux measurements and meteorological data, Keenan *et al.* (2013) found a substantial increase of 1.07 ± 0.3 hPa g C kg H_2O^{-1} yr^{-1} in IWUE in temperate and boreal forests of the northern hemisphere over the past two decades; this is related to increasing GPP and decreasing ET. However, different responses in water-use efficiency are found when upscaling from leaf to ecosystem level, suggesting feedbacks through boundary layer mixing of moist air (Field *et al.*, 1995), root allocation and leaf area index changes (Piao *et al.*, 2007; Norby & Zak, 2011), and structural changes in ecosystems (Cramer *et al.*, 2001). For instance, rising CO_2 concentration is expected to enhance leaf area index (LAI) (Norby & Zak, 2011) and increase ET from canopy transpiration and interception (Betts *et al.*, 1997; Piao *et al.*, 2007). On the other hand, increased LAI also causes a decline in the fraction of solar radiation reaching the soil surface and decreases the bare soil evaporation, which may downregulates ET (Hungate *et al.*, 2002).

Climate change may locally offset the effects of CO_2 fertilization on EWUE. Under climate warming, both modeling and experimental studies agree that EWUE should decrease, mainly due to an enhancement in ET under temperature-driven increasing vapor pressure deficit (De Boeck *et al.*, 2006; Bell *et al.*, 2010; Niu *et al.*, 2011). Response of EWUE to changes in precipitation depends upon the extent to which the system is water limited, with the EWUE of wetland and cropland decreasing with increasing precipitation, and that of forest and grassland ecosystems behaving oppositely (Tian *et al.*, 2010). However, extrapolating the results of these detailed studies to large area is complex. Firstly, across ecosystems, GPP can be decoupled from ET due to the variable partitioning of the surface energy budget into water and heat losses (Nemani *et al.*, 2003; Ponton *et al.*, 2006; Gao *et al.*, 2007). Secondly, the responses of EWUE depend on relative changes of GPP compared to ET driven by variations of different climatic factors (e.g., temperature, precipitation, radiation, and so forth) (Niu *et al.*, 2011; Zhu *et al.*, 2011). Climate change should produce different responses in EWUE and to varying degrees. For example, based on the Integrated Biosphere Simulator (IBIS), Zhu *et al.* (2011) concluded that EWUE varies between different geographic regions in China with negative effects of climate change mainly in southern regions but positive impacts in northern China and mountain regions.

In addition to limits imposed by CO_2 and climate, the productivity of many global ecosystems is limited by lack of nitrogen (and phosphorus), particularly those outside the tropics (Norby *et al.*, 2010; Wang *et al.*, 2010; Zhang *et al.*, 2014). According to Norby *et al.* (2010), the enhancement of Net Primary Production (NPP) under elevated CO_2 declined from ~24% in 2001–2003 to ~9% in 2008 due to declining nitrogen availability at the Oak Ridge FACE forest experiment. The impact of nitrogen deposition resulting from human activities has been of particular significance due to the large additional amounts of reactive nitrogen (NH_3 and NO_x) entering ecosystems (Sun *et al.*, 2010). For example, in China, Liu *et al.* (2013) found an average annual increase of 0.41 kg N ha^{-1} between 1980 and 2010, due to rapid agricultural, industrial, and urban development. Increased deposition of reactive nitrogen may stimulate photosynthetic rates and thus vegetation growth, at least initially, in nitrogen-limited ecosystems (Livingston *et al.*, 1999; Mitchell *et al.*, 2003; Granath *et al.*, 2009). Dordas & Sioulas (2008) found that nitrogen application during 2 years to safflower crops increased carbon assimilation rates by an average of ~51% and stomatal conductance to water vapor by ~27%, but with a net effect being an enhancement of leaf-level WUE by ~60% compared to nonfertilized plots. Jennings (2013) reached a similar conclusion for a temperate deciduous forest in the northeast of the USA, with higher leaf WUE_i through increased photosynthetic rates in response to nitrogen fertilization.

Tree-ring isotopes and remote-sensing datasets have the advantage to consider real-world, large-scale vegetation, and long-term changes, but there are experienced difficulty in quantifying the responses of EWUE to a single driver among multiple covarying factors (Cramer *et al.*, 2004; Hietz *et al.*, 2005; Nock *et al.*, 2011; Peñuelas *et al.*, 2011; van der Sleen *et al.*, 2015). Manipulation experiments can be used to isolate single drivers, for example, CO_2, climate and nutrients, but are being short-term and not fully able to capture long-term ecosystem adaptation or large-scale atmospheric feedbacks (Feng, 1999). Moreover, conclusions drawn from site level studies can be sensitive to the specific climatic and soil condition and are not easily extrapolated to larger spatial scales. Process-based ecosystem models, while far from being fully inclusive of the processes that control EWUE (e.g., species shifts), are about the only tool that can scale up theory to the planetary scale and isolate effects from different drivers by simulations. Thus, it is critical to compare the observed responses of EWUE from field experiments with the predictions from ecosystem models.

The purpose of this study was to investigate EWUE trends over the globe during the 1982–2008 time period. To do this, we will apply a statistical model to partition and attribute EWUE trends to separate environmental drivers. Although real-world ecosystems are influenced by many factors such as management, disturbance, species change, and climate, global models do not include all these interactions and their simulations can currently only distinguish EWUE trends to climate change ('CLIM'), rising CO_2 ('CO_2'), and nitrogen deposition ('NDEP'). These three different scenarios are simulated by an ensemble of carbon cycle models to quantify the separate driver effects on EWUE. Partial correlation analysis is also conducted to have a deeper understanding of relationships between EWUE and climatic variables.

Materials and methods

Process-based models and simulations

We used gross primary production (GPP) and evapotranspiration (ET) output from four process-based carbon cycle models run at 0.5 degree resolution and hereafter called DGVM (even though not all the models included active vegetation dynamics in the simulations). The four models (CLM4CN, CABLE, LPJ, and ORCHIDEE) differ in how they represent physical processes (Table S1), and they therefore produce different responses in GPP and ET to changes in external drivers. All the models were forced using the same observed climatic variables from the CRU-NCEP version4 product. CO_2 concentration data were taken from ice-core measurements, and land use was fixed at 1850 conditions.

Two models, LPJ and ORCHIDEE, do not include an interactive nitrogen cycle; therefore, the only simulations possible over the last century were as follows:

- S1: elevated atmospheric CO_2 concentrations with other factors kept constant.
- S2: elevated atmospheric CO_2 concentrations and climate change.

Thus, for the above two models, the influence of CO_2 enrichment ('CO_2') on GPP, ET, and EWUE can be estimated from Simulation S1. The effect of climate change ('CLIM') can be separated by the difference of simulations S2 and S1.

For CABLE, it is also possible to simulate:

- S3: elevated atmospheric CO_2 concentrations, climate change as well as the impacts of nitrogen deposition.

The effect of nitrogen deposition ('NDEP') can then be separated by the difference of simulations S3 and S2.

For CLM4CN, scenario 'CLIM' considered the impact of varying climate only on GPP and ET, holding constant all other factors. Effects of 'CO_2' and 'NDEP' can be quantified from the difference with a control run 'CTRL', which used stable climate conditions, repeating years between 1901 and 1920 with all other forcing kept constant (Mao *et al.*, 2013). The combined impacts of CO_2, climate change, and nitrogen deposition were derived by adding the EWUE trends estimated from the 'CO_2', 'CLIM', and 'NDEP' scenarios together.

Data-driven model

Global datasets of estimated gross primary productivity (GPP) and evapotranspiration (ET) from model tree ensemble (MTE) were downloaded from the Department of Biogeochemical Integration (BGI) of MPI (http://www.bgc-jena.mpg.de/geodb/projects/Data.php). The MTE model was written by Jung *et al.* (2009, 2011) at 0.5° spatial resolution and a monthly temporal resolution from 1982 to 2008, using monthly FLUXNET eddy-covariance sites. It is a statistical model that interpolates flux tower measurements of GPP and ET using satellite fraction of absorbed photosynthetic active radiation (fAPAR) global time varying maps, climate fields, and land-cover datasets (Jung *et al.*, 2011).

Analysis

Ecosystem annual mean water-use efficiency (EWUE) is defined by Eqn (1), widely used in previous studies to estimate EWUE (e.g., Ponton *et al.*, 2006; Hu *et al.*, 2008; Yu *et al.*, 2008; Beer *et al.*, 2009; Zhu *et al.*, 2011):

$$\mathrm{EWUE} = \frac{\mathrm{GPP}}{\mathrm{ET}} \quad (1)$$

where GPP refers to annual gross primary productivity (g C m^{-2}) and ET to annual evapotranspiration (mm) in each pixel as given by the MTE and DGVMs.

Although GPP and ET output from DGVMs cover the last century, we selected just the last three decades (1982–2008) for calculating EWUE trends because this is the period covered by the MTE model. Monthly, GPP and ET datasets from each gridded dataset from DGVM and MTE were firstly aggregated to annual values. Pixels with mean annual NDVI (AVHRR NDVI3 g dataset) less than 0.1 were masked in subsequent analysis (Zhu *et al.*, 2013). We then calculated global mean EWUE as the ratio of global mean GPP and global mean ET for each year over the period 1982–2008. Series with missing values in the analysis period were excluded from the temporal trend analysis. The trend was obtained using Theil–Sen linear regression of EWUE vs. year, a method for robust linear regression that chooses the median slope among all linear fits through pairs of two-dimensional sample points (Sen, 1968). The average trend of each variable for one scenario was calculated as the arithmetic mean value of the trends estimated by different DGVMs for the same scenario. The uncertainty is defined as the error of the average trend and computed as the standard deviation of the trends of each DGVM. Apart from global mean EWUE trends, we examined the Theil–Sen linear regression slope of EWUE at the per-pixel level as well.

To compare the response of variations of EWUE to annual mean temperature, precipitation (CRU TS 3.21, Harris *et al.*, 2014), and solar downward radiation (CRU-NCEP version 4 product), partial correlation analysis was carried out for each pixel for the MTE model and S2 (CLIM + CO_2) of DGVMs. Partial correlation provides the correlation between the interannual fluctuation in EWUE and that in each of the three climatic factors while controlling for the other two. Following Peng *et al.* (2013), long-term linear trends were removed from both the EWUE series and climatic series before partial correlation analysis was conducted.

Results

Global EWUE trends

Trends of global EWUE from MTE and DGVM (g C m^{-2} mm^{-1} yr^{-1}) during 1982–2008 are shown in Fig. 1. According to the DGVM approach, our regression analysis found that increasing CO_2 concentration explains most of the global EWUE trend, followed by climate change and nitrogen deposition. In the MTE approach, these drivers were not explicitly separated.

For the 'CO_2' storyline, EWUE trends are observed to increase significantly for all DGVMs, with an average rate of 0.0056 ± 0.0025 (mean ± standard deviation across models) g C m^{-2} mm^{-1} yr^{-1}. CABLE produces the largest positive trend of 0.0085 g C m^{-2} mm^{-1} yr^{-1} ($P < 0.01$) and CLM4CN the smallest (0.0025 g C m^{-2} mm^{-1} yr^{-1}, $P < 0.01$). For the 'CLIM' storyline, the average EWUE trend is close to zero within its uncertainty (0.0007 ± 0.0013 g C m^{-2} mm^{-1} yr^{-1}). The 'CLIM' storyline from CLM4CN, LPJ, and ORCHIDEE shows significant increases (0.0015, 0.0008, 0.0016 g C m^{-2} mm^{-1} yr^{-1}, respectively, $P < 0.01$), while CABLE indicates a decreasing trend (−0.0011 g C m^{-2} mm^{-1} yr^{-1}, $P < 0.01$). The 'NDEP' storyline shows a near-zero EWUE trend. CLM4CN had a positive value of 0.0004 g C m^{-2} mm^{-1} yr^{-1} ($P < 0.01$), while CABLE produced a negative trend of −0.0004 g C m^{-2} mm^{-1} yr^{-1} ($P < 0.01$). EWUE trends from 'CLIM+CO_2+NDEP', with the three drivers together, show significant increases over the last 30 years, with an average value of 0.0064 ± 0.0017 g C m^{-2} mm^{-1} yr^{-1} ($P < 0.01$). In contrast, EWUE trends from the MTE approach show a decreasing trend of −0.0006 g C m^{-2} mm^{-1} yr^{-1}, but this is not statistically significant ($P > 0.05$).

Although DGVM simulations S1 and S2 all agree on increasing EWUE during the study period, they differ with each other in terms of GPP and ET. According to Fig. 2a, climate change and rising CO_2 ('CLIM+CO_2', Simulation S2) produces both increasing GPP and increasing ET. On average, GPP in S2 increases from 1335 g C m^{-2} yr^{-1} to 1431 g C m^{-2} yr^{-1} and ET increases from 676 mm yr^{-1} to 685 mm yr^{-1} between the first five and the last 5 years (Fig. 2a). In the CO_2, only simulation S1, ET averaged across all DGVMs remains almost constant (from 714 mm yr^{-1} averaged during 1982–1986 to 712 mm yr^{-1} averaged during

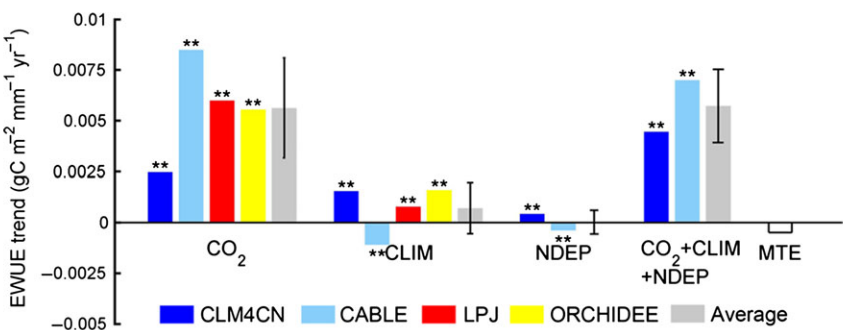

Fig. 1 WUE trends (g C m^{-2} mm^{-1} yr^{-1}) estimated by MTE model and DGVMs at global scale from 1982 to 2008. DGVM scenario simulations include 'CO_2' (S1), 'CLIM' (S2-S1), 'NDEP' (S3-S2), and 'CLIM+CO_2+NDE'. ** indicates statistically significant at the 99% ($P < 0.01$) level and * statistically significant at the 95% ($P < 0.05$) level. The average trend of each model scenario was calculated as the arithmetic mean value of the trends estimated by different DGVMs, and the error bar of the average trend was computed as the standard deviation of the trends of each DGVM.

2004–2008), and GPP increases from 1310 g C m^{-2} yr^{-1} to 1393 g C m^{-2} yr^{-1} (Fig. 2b). The effect of climate change ('CLIM') alone, estimated from the difference between S1 and S2 for each model, is thus to increase ET in all models (Fig. 2c). The ET trend from 'CLIM' is on average positive (0.63 ± 0.17 mm yr^{-2}), ranging between 0.52 mm yr^{-2} in LPJ and 0.88 mm yr^{-2} for CLM4CN.

Spatial variations of MTE and DGVM-based EWUE trends

The global mean EWUE trend from the four DGVMs is significantly higher than that from MTE-based estimate, as shown in Fig. 1. Here, spatial variations of the sensitivities of the trends of EWUE, GPP, and ET in response to CO_2, climate, and nitrogen deposition and to all drivers are shown in Fig. 3.

Results from DGVM simulations show that CO_2 alone produces an increase of EWUE in most pixels (~99%); of these, ~82% are statistically significant (Panel a1 in Fig. 3). CO_2 increase alone increases GPP and reduces ET in over 70% pixels, mainly in North America, South America, central Africa, Europe, west Siberian lowlands, central Siberia, southeastern China, and Southeast Asia (Panel b1 in Fig. 3).

Climate change alone (S2-S1) results in EWUE increasing at high latitudes (Alaska, Canada, northern Eurasia), southern and eastern Africa, southwestern China, and Southeast Asia, but EWUE decrease in the Amazon Basin, parts of western North America, central and southern Africa, southwestern and eastern Australia, southeastern Europe, and northeast Asia.

Increase in atmospheric nitrogen deposition has much smaller effect on EWUE trend than CO_2 or climate change over the same period. The EWUE trends in response to NDEP are positive for ~60% of land pixels, with decreasing EWUE-NDEP primarily in west Siberia, eastern Europe, the United States, northern Canada, parts of the Amazon Basin, and southeastern China.

When the effects of all three drivers are combined, Fig. 3a shows positive EWUE trends from DGVMs in ~91% of pixels and negative ones only over the Amazon Basin, parts of Alaska, small parts of Africa and East Asia, and parts of eastern Australia. The MTE model gives a different picture (Panel a5 in Fig. 3), with only 52% of the pixels showing an increase of EWUE (northern Canada, the United States, eastern and southeastern Europe, the Indian, northern China and Sahel), and ~24% of them are statistically significant. Areas with negative trends of EWUE-MTE are widespread in North America (Alaska and parts of Canada), the Amazon Basin, central Africa, western Europe, Siberia, Southeast Asia, and Australia. Compared with spatial patterns of DGVMs results with all drivers varied, the percentage of pixels with increasing GPP and decreasing ET of EWUE-MTE trends is much lower. Therefore, the positive responses of GPP to the combined changes in CO_2, climate, and nitrogen deposition as simulated by DGVMs are much stronger and spatially broader than those by the MTE method.

Partial correlations between EWUE and climate factors

Partial correlations between annual fluctuations of climatic variables (mean annual temperature, total annual precipitation, and mean annual solar downward radiation) and anomalies of EWUE were analyzed for MTE and DGVM models (S2). The patterns are consistent between the two approaches, as shown below.

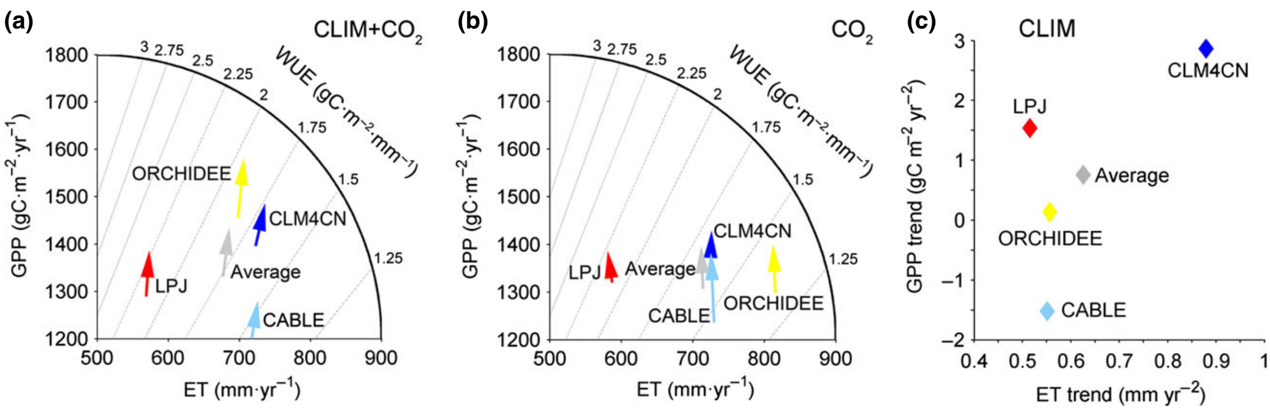

Fig. 2 Changes in global mean GPP and ET in different model simulations. In Panel (a) and (b), the arrow starts at the mean GPP (ET) during 1982–1986 and points to the mean GPP (ET) during 2004–2008 under different factorial model simulations with different fixed drivers: (a) combined effects of climate change and rising CO_2 (S2); (b) rising CO_2 only (S1). Panel (c) shows the temporal linear trend of GPP vs. the linear trend of ET induced by climate change (CLIM) alone for each DGVM during 1982–2008.

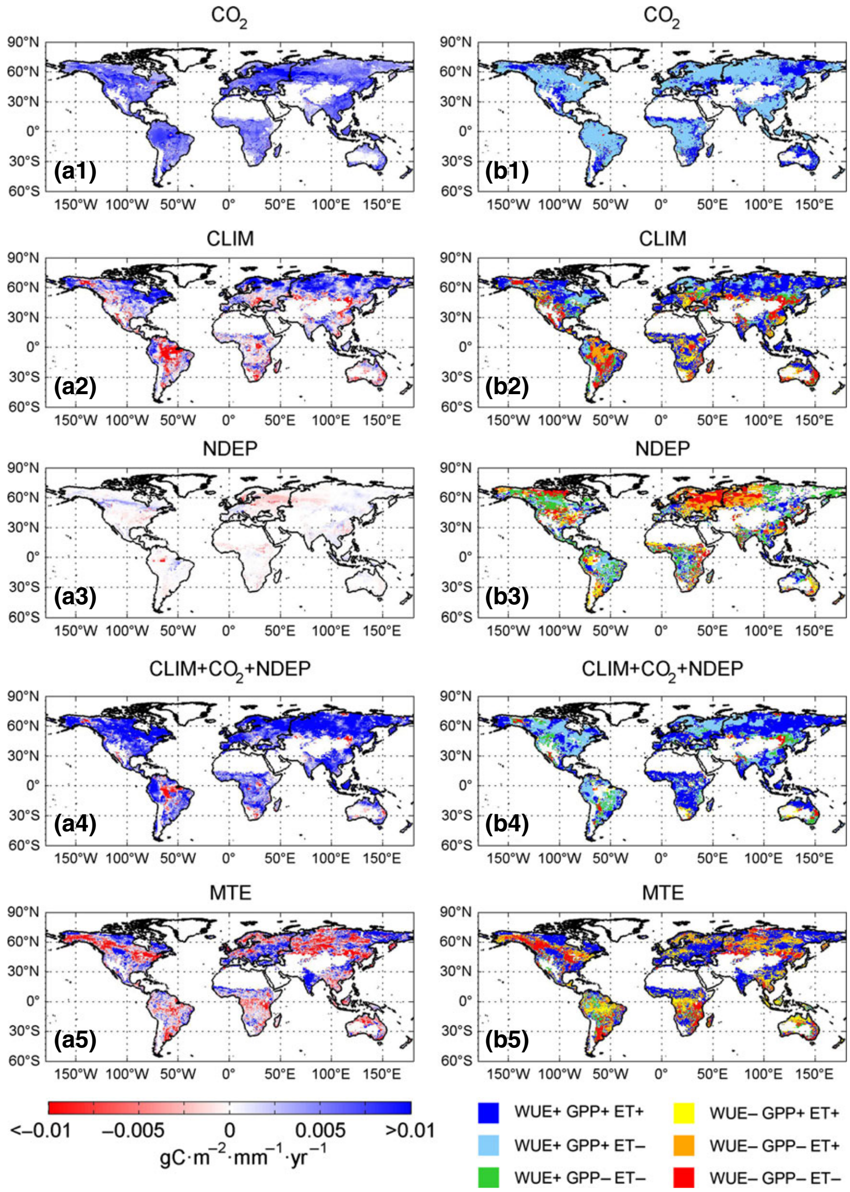

Fig. 3 Spatial patterns of (a) WUE trends and (b) composite maps of the sign of GPP and ET trends from DGVMs simulation (1) 'CO_2' (S1); (2) 'CLIM' (S2-S1); (3) 'NDEP' (S3-S2); (4) 'CLIM+CO_2+NDEP' and (5) from the MTE empirical model. In Panel (b), the symbol '+' represents positive WUE (GPP or ET) trend, while '-' refers to negative WUE (GPP or ET) trend during the study period.

Figure 4a provides the spatial distributions of partial correlation coefficients between annual fluctuations of mean annual temperature and EWUE. The responses of variation of EWUE are consistent between DGVMs and MTE. Positive correlations are found mainly in the high latitudes, suggesting that warmer years have positive EWUE in these regions. EWUE is negatively correlated with temperature in southern and central Africa, South America, southeastern North America, south Asia, and northern and eastern Australia.

Figure 4b suggests similar patterns of the partial correlations between EWUE and total annual precipitation for MTE and DGVMs. EWUE is positively correlated with precipitation in lower latitudes such as Central America, South America and western Africa, the Mediterranean coast and central Asia, and is negatively correlated with precipitation only in high latitudes/high elevation regions such as the Qinghai–Tibetan Plateau.

Responses of EWUE to mean annual radiation are also consistent between MTE and DGVMs (Fig. 4c). Positive correlations are mainly observed in northern Canada and eastern Siberia, while negative correlations appear primarily in the United States, parts of South

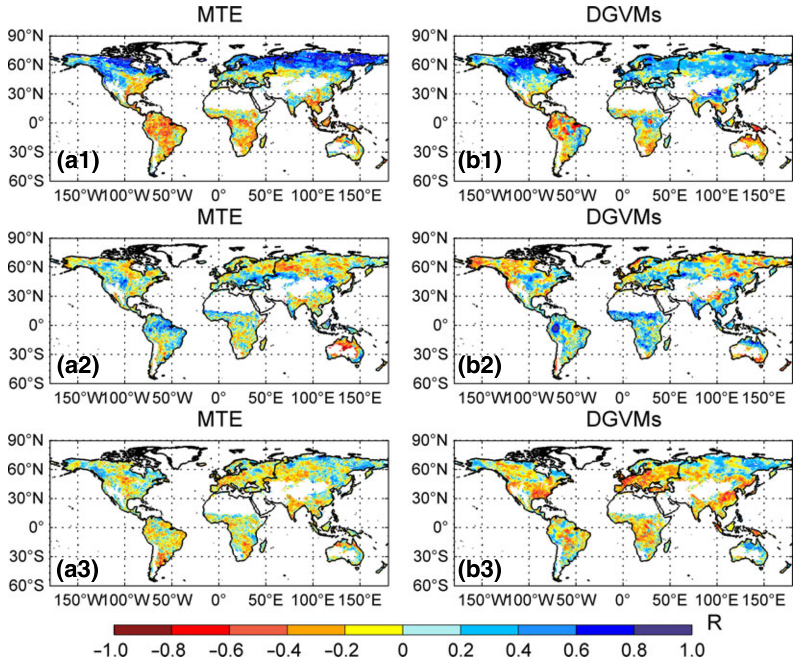

Fig. 4 Spatial patterns of partial correlation coefficients between (a) annual mean temperature, (b) annual precipitation, (c) annual mean solar downward radiation and WUE resulting from (1) MTE model and (2) DGVM simulation S2.

America, central Africa, southeastern China, the Indian subcontinent, Europe, and western Siberia.

Discussion

Comparisons of MTE and DGVM-simulated EWUE trends

The differences between EWUE trends from DGVMs and MTE may originate from nonmodeled CO_2 physiological effects on stomatal conductance in the MTE algorithm (Jung *et al.*, 2010). Jung *et al.* (2009) employed a model tree ensemble machine-learning algorithm by integrating point-wise ET measurements at the FLUXNET observing sites with geospatial information from satellite observation (fAPAR) and surface meteorological data (potential radiation, temperature, and precipitation). The physiological impacts on leaf stomata of rising atmospheric CO_2 via stomatal closure mechanisms are excluded in the model tree training and upscaling of ET datasets, while the structural impacts (e.g., changes in LAI) is supposed to be taken into account through the variation of fAPAR (Jung *et al.*, 2009, 2011). Thus, the EWUE trends from the MTE approach should be closer to those estimated in the 'CLIM' (S2-S1) simulation than to S2.

Previous studies have concluded that vegetation interacts with atmospheric CO_2 concentration mainly in two ways – the physiological responses and the structural responses. Whether elevated CO_2 alone will set an upward or downward trend in water-use efficiency depends on which responses dominate.

When the physiological responses dominate plants tend to reduce stomatal conductance under high CO_2 levels and reduce transpirational water loss more than CO_2 assimilation (Ball *et al.*, 1987; Field *et al.*, 1995; Berry *et al.*, 2010; Chapin *et al.*, 2011); this results in a positive contribution to water-use efficiency (Keenan *et al.*, 2013). Reductions in stomatal conductance induced by this physiological response are typically 20–40% (Field *et al.*, 1995; Betts *et al.*, 1997; Medlyn *et al.*, 2001; Leipprand & Gerten, 2006), a significant decrease in transpiration. Betts *et al.* (1997, 2000) employed the Hadley Centre general circulation model and concluded that the physiological responses of vegetation under doubled CO_2 concentration leads to a general reduction in daytime mean canopy conductance by ~5.7% globally. Here, we also examined the stomatal regulation of elevated CO_2 using the ratio of transpiration (TR) to LAI (TR/LAI) in S1 simulation over the last three decades (Fig. S1), which is consistent with stomatal conductance decrease under elevated CO_2 in observation (Medlyn *et al.*, 2001; Wullschleger *et al.*, 2002; Long *et al.*, 2004; Ainsworth & Rogers, 2007).

When the structural responses dominate, higher CO_2 leads to greater leaf area index (Ball *et al.*, 1987; Drake & Gonzàlez-Meler, 1997; Kergoat *et al.*, 2002), which potentially offsets stomatal closure per leaf area (Hungate *et al.*, 2002; Betts *et al.*, 2007; Zhu *et al.*, 2012). A global increase in LAI of ~7.2% due to increased productivity under higher CO_2 levels was found by Betts *et al.* (1997). Piao *et al.* (2007) also found that because increased LAI in response to CO_2 provides a greater cumulative surface area for canopy water transpiration and rainfall interception, the rate of annual ET is enhanced by ~0.08 mm yr^{-2}. At the same time, increased LAI under CO_2 enrichment can lead to reduction of the amount of solar radiation reaching the soil surface, reducing soil evaporation (Hungate *et al.*, 2002). This latter process may to some extent offset the greater amount of ET resulting from greater LAI.

During the study period, GPP estimated by the four DGVMs is simulated to increase, while ET showed a slight decline (Fig. 2b), producing a significantly increasing multi-model averaged EWUE trend (Fig. 1). This result is in agreement with previous studies that overall the direct effect of elevated CO_2 levels on stomatal conductance dominates over its impacts on vegetation structure (Betts *et al.*, 1997; Hungate *et al.*, 2002; Leipprand & Gerten, 2006; Felzer *et al.*, 2009). But the dominant effect of CO_2 is not uniform across the globe, because the balance between the structural and physiological responses varies regionally (Leipprand & Gerten, 2006). For example, in drier areas such as Australia, Central America, as well as parts of eastern Siberia, India, southeastern Europe, southern Africa, and South America, evapotranspiration tends to increase (Panel a in Fig. S2). This increase is due to the obvious rise in transpiration (Panel c in Fig. S2), which is positively correlated with increased LAI in these areas (Panel d in Fig. S2). Using the LPJ model, Leipprand & Gerten (2006) simulated an expansion of vegetation coverage in dry regions under higher CO_2 that caused an increase of transpiration offsetting the physiological effect.

Neglecting the effects on the leaf energy balance, Piao *et al.* (2007) concluded ignoring the indirect physiological effect of higher CO_2 on the energy balance (higher leaf temperature from stomatal closure), the ecosystem transpiration change that accompanied the preindustrial to current change in CO_2 level can be separated into effects of changes in LAI (structural effects) and of stomatal conductance (physiological effects). To test the hypothesis that nonmodeled CO_2 physiological effects in the MTE model explain why this approach does not have a persistent increase of ET trends during 1982–2008, and even a recent decrease (Jung *et al.*, 2010), we write evapotranspiration (ET) using the identity:

$$\mathrm{ET} = \mathrm{LAI} \times \frac{\mathrm{ET}}{\mathrm{LAI}} \tag{2}$$

The term ET/LAI represents ET per unit of LAI as a surrogate for transpiration (TR) per unit of LAI, that is, TR/LAI. TR/LAI approximately quantifies the stomatal conductance (g_s). Furthermore, stomatal aperture being generally optimized to maximize carbon gain for a unit loss of water (Katul *et al.*, 2009) under elevated CO_2, carbon assimilation can be maintained at the original level even if g_s is reduced (Chapin *et al.*, 2011; Zhu *et al.*, 2011). Thus, we assumed that the nonmodeled physiological effect of CO_2 by the MTE model does not lead to a bias in the estimation of GPP, and we did not write GPP using an identity similar to Eqn (2). We calculated the ratio of global mean EWUE during 2004–2008 ($\mathrm{EWUE}_{04\text{-}08}$) to 1982–1986 ($\mathrm{EWUE}_{82\text{-}86}$) in Eqn (3):

$$\frac{\mathrm{EWUE}_{04-08}}{\mathrm{EWUE}_{82-86}} = \frac{\frac{\mathrm{GPP}_{04-08}}{\mathrm{ET}_{04-08}}}{\frac{\mathrm{GPP}_{82-86}}{\mathrm{ET}_{82-86}}} = \frac{\mathrm{GPP}_{04-08}}{\mathrm{GPP}_{82-86}} \times \frac{\mathrm{LAI}_{82-86} \times \left(\frac{\mathrm{ET}}{\mathrm{LAI}}\right)_{82-86}}{\mathrm{LAI}_{04-08} \times \left(\frac{\mathrm{ET}}{\mathrm{LAI}}\right)_{04-08}} \tag{3}$$

We obtained a value of 0.999 for k = $\mathrm{EWUE}_{04-08}/\mathrm{EWUE}_{82-86}$ using the MTE results, indicating a very stable EWUE between 1982 and 1986 and 2004–2008 in this model. Nevertheless, due to ignorance of the influence of rising CO_2 on g_s, the MTE approach assumed $[(\mathrm{ET}/\mathrm{LAI})_{82-86}]/[(\mathrm{ET}/\mathrm{LAI})_{04-08}]$ as 1. In practice, it should be larger than 1 as a result of partial closure of stomata under the higher CO_2 conditions of the later period. So, we estimated global mean $[(\mathrm{ET}/\mathrm{LAI})_{82-86}]/[(\mathrm{ET}/\mathrm{LAI})_{04-08}]$ (termed λ) as 1.050 using DGVM Simulation S1. Then, the theoretical ratio between $\mathrm{EWUE}_{04\text{-}08}$ and $\mathrm{EWUE}_{82\text{-}86}$ (k′) can be calculated from k multiplied by λ above, and this gives a value of 1.048, suggesting a theoretical potential increase in EWUE if the effects of elevated CO_2 on stomatal conductance and LAI are both taken into consideration. The value of k′ is consistent with the increasing trend in EWUE estimated by model scenario 'CLIM + CO_2 + NDEP'. Comparison of the spatial distribution of parameter k and k′ (Fig. S3) also suggested that without the effects of atmospheric CO_2, ~63% pixels indicate a decrease in EWUE, whereas taking effects of stomatal regulation into consideration, ~74% pixels undergo an enhanced EWUE during the study period.

Spatial patterns of responses of EWUE to climate variables

Ecosystem-scale water-use efficiency responds to the variations of climatic factors. Different EWUE behaviors have been observed across different ecosystems (Fig. 4) as a result of variation in environmental conditions and in the physiological characteristics of vegetation communities (Ponton *et al.*, 2006; Zhu *et al.*, 2011).

Regions with positive interannual responses of EWUE to the changes of annual mean temperature are in the high latitudes (Fig. 4a). A lengthening of the growing season is consistent with warming, especially at higher latitudes. Tucker *et al.* (2001) reported an advance in the start of the growing season of 5.6 and 1.7 days during 1982–1991 and 1992–1998, respectively, at higher northern latitudes, which were both associated with global warming. Zhou *et al.* (2001) also found that the growing-season length has increased by 18 days in Eurasia and 12 days in North America from 1981 to 1999, which is caused by earlier spring and later autumn. As the length of the growing season has increased due to the increase in surface air temperature (Körner & Basler, 2010; Gunderson *et al.*, 2012), the amount of both GPP and ET increases over the study period. Nevertheless, the photosynthetic rates are also directly accelerated by warming (Gunderson *et al.*, 2000; Flanagan & Syed, 2011), while the evapotranspiration rates tend to remain unchanged due to stomatal regulation (Serrat-Capdevila *et al.*, 2011). Consequently, the faster increase of GPP compared to ET leads to a positive trend of EWUE at high latitudes in response to warming. In contrast, in relatively wetter areas (such as southeastern America, the Amazon Basin, and Southeast Asia), increasing temperature causes a negative effect on simulated EWUE. With abundant precipitation, an increase in temperature in these regions will increase ET (by reducing the latent heat for vaporization) more significantly than GPP (Zhu *et al.*, 2011), thus leading to a reduction in EWUE.

Contrary to temperature, changes of EWUE are negatively correlated with annual precipitation in most parts of high northern latitudes (Fig. 4b), where cold winter temperature and cloudy summers are the primary limitations for vegetation growth (Nemani *et al.*, 2003). Mazzarino *et al.* (1991) found that nitrogen mineralization is positively correlated with both soil moisture and temperature, thus increasing precipitation should increase available nitrogen for plant uptake there. However, if temperature does not rise concurrently with precipitation, nitrogen availability may not increase, and EWUE may not increase because GPP is nitrogen limited. Moreover, increasing precipitation during the nongrowing season could also aggravate nitrogen limitation due to enhanced nitrogen leaching and denitrification (Hovenden *et al.*, 2014), resulting in a reduction in GPP, and declining water-use efficiency. Positive partial correlations of EWUE and precipitation mainly occur in warmer and (or) drier areas, where water is the explicit limitation on primary productivity (Knapp & Smith, 2001; Nemani *et al.*, 2003; Bai *et al.*, 2008). In these areas, higher annual precipitation can remarkably improve the productivity of individual plants (Niu *et al.*, 2011; Zhu *et al.*, 2011) and then enhance GPP, forcing a positive relationship between EWUE and annual precipitation.

Pieruschka *et al.* (2010) pointed out the positive near-linear relationship between the absorbed energy and both canopy conductance and transpiration. Hence, although increasing radiation is thought to result in increasing GPP (Gitelson *et al.*, 2008), the larger responses of canopy transpiration (Gates, 1964; Pieruschka *et al.*, 2010) and soil evaporation eventually give rise to declining EWUE trends with increasing solar radiation in mid and low latitudes (Fig. 4c). In comparison, in relatively high latitudes, especially eastern Siberia, vegetation productivity is limited by available solar radiation during summer (Nemani *et al.*, 2003). Hence, increases in solar radiation stimulate GPP much more markedly than ET and eventually result in an enhanced EWUE (Fig. 4c).

Ecosystem water-use efficiency in different definitions

At leaf level, water-use efficiency (WUE) is usually defined as the ratio of carbon assimilation (A) and transpiration (Keenan *et al.*, 2013). However, carbon assimilation and transpiration cannot be quantified through direct measurements (Beer *et al.*, 2009) when scaling up from leaf to ecosystem level. Previous studies concluded that global evapotranspiration is dominated by canopy transpiration, although the ratio of transpiration to total evapotranspiration ranges from 48% to 90% (Gerten *et al.*, 2005; Cao *et al.*, 2010; Haverd *et al.*, 2011; Jasechko *et al.*, 2013), depending on vegetation coverage, surface wetness, and the availability of soil moisture for vegetation roots to take up water (Wang & Dickinson, 2012). Hence, many studies have defined EWUE as GPP divided by ET as the substitute for ecosystem-level A and transpiration. Nevertheless, as ET contains soil evaporation (ES), wet-canopy evaporation (EC), and canopy transpiration (TR), trends in ES and EC may contribute to the trend of water-use efficiency. To investigate the contribution of bare soil and canopy evaporation trends on EWUE, we also calculated transpiration-based WUE (WUE_t) as the ratio of GPP and TR (Fig. 5) for each DGVM. Consistent with EWUE, scenario 'CO_2' displays a significant increasing global mean WUE_t trend and simulation 'NDEP' produced a near-zero WUE_t trend. But compared with EWUE, which displays a rather small increase due to climate change (Fig. 1), WUE_t clearly shows declining trends. This phenomenon can be explained by the decreasing trends of evaporation as observed in different regions globally (Golubev *et al.*, 2001; Liu *et al.*, 2004; Hobbins *et al.*, 2004; Rayner, 2007; Roderick *et al.*, 2007). These trends may result from: firstly, declining global solar irradiance resulting from changes in cloudiness or aerosol concentration (Roderick & Farquhar, 2002; Liu *et al.*, 2004); or secondly, decreases in terrestrial mid-latitude near-surface wind speed (Rayner, 2007; Roderick *et al.*, 2007, 2009). Therefore, with the impacts of soil evaporation and interception eliminated, enhancement of TR owing to climate change markedly exceeds that of GPP, resulting in an evident reduction in WUE_t.

A nonlinear decreasing empirical relationship between water-use efficiency and vapor pressure deficit (VPD) was observed by many studies at both leaf and ecosystem level (Baldocchi *et al.*, 1987; Tang *et al.*, 2006; Linderson *et al.*, 2012), causing differences between sites and regions that are only reflecting trends of VPD. To remove the effects of VPD for a multi-site analysis, Beer *et al.* (2009) introduced the definition of inherent water-use efficiency, IWUE (defined as the product of vapor pressure deficit and EWUE, that is, GPP·VPD/ET); at ecosystem level, they found a stronger relationship between GPP and ET·VPD than between GPP and ET. Based on this, we calculated transpiration-based inherent water-use efficiency ($IWUE_t$) as GPP·VPD/TR in our study to minimize the effect of VPD. Similarly to EWUE and WUE_t, for simulation 'CO_2', $IWUE_t$ increases significantly while simulation 'NDEP' shows a decline in $IWUE_t$ during the study period. Under climate change alone, all models agree on a decreasing trend of global mean $IWUE_t$. And the combined scenario 'CLIM + CO_2 + NDEP' displays an increasing $IWUE_t$ trend, which is consistent with EWUE and WUE_t.

In summary, to our knowledge, this study is the first one to comprehensively detect changes of EWUE on a worldwide scale and to attribute EWUE trends to separate environmental drivers. Our study has also pointed out the potential systematic error in the trend of empirical-model ET products due to nonmodeled physiological effects of rising atmospheric CO_2 concentration, which should be fully considered in order to reduce their uncertainties. Nevertheless, the model simulations available for this study do not fully allow to quantify the nonlinear interactions between different factors. For instance, the interaction between different climate, land use, and CO_2 is not considered when estimating the effect of climate change alone based on the difference of simulations S2 and S1. More simulations are needed to characterize these interactive effects of environmental drivers on EWUE.

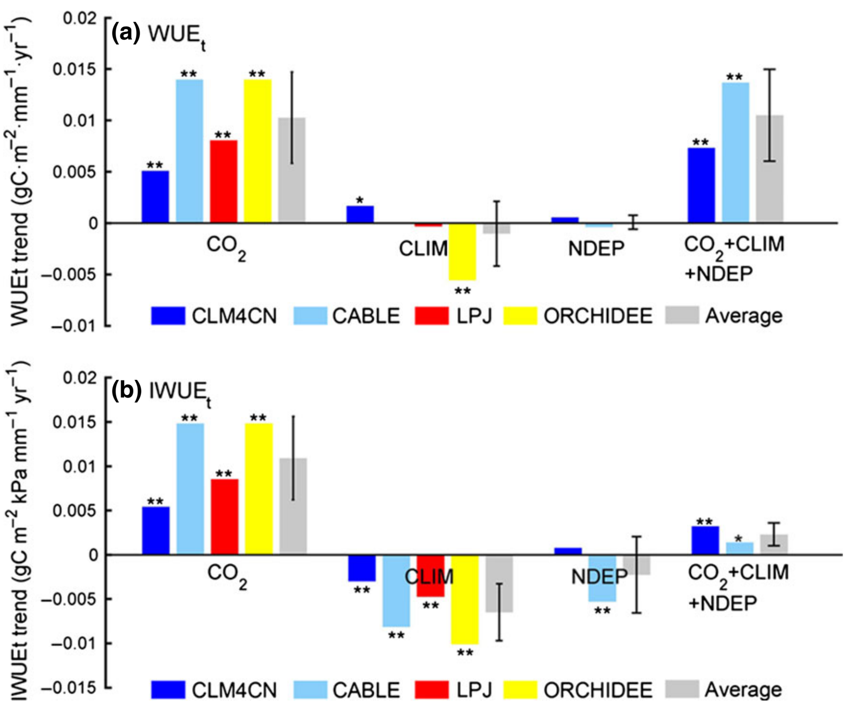

Fig. 5 Model-simulated (a) transpiration-based WUE (WUE_t) trends (g C m^{-2} mm^{-1} yr^{-1}) and (b) transpiration-based inherent WUE ($IWUE_t$) trends (g C m^{-2} kPa mm^{-1} yr^{-1}) at global scale from 1982 to 2008. Model scenario simulations include DGVM simulation 'CO_2' (S1), 'CLIM' (S2-S1), 'NDEP' (S3-S2), and 'CLIM+CO_2+NDEP'. ** indicates statistically significant at the 99% ($P < 0.01$) level, and * statistically significant at the 95% ($P < 0.05$) level. Here, VPD (kPa) is the daytime vapor pressure deficit during the growing season derived from hourly temperature, specific humidity, and surface pressure datasets from the Global Monitoring and Assimilation Office (GMAO, ftp://goldsmr2.sci.gsfc.nasa.gov/data/s4pa/MERRA/MAT1NXSLV.5.2.0/) (Zhao *et al.*, 2005; Zhao & Running, 2010).

Acknowledgements

We thank Dr. Jung for satellite derived ET and GPP product. This study was supported by the National Natural Science Foundation of China (41125004), Chinese Ministry of Environmental Protection Grant (201209031), the 111 Project (B14001), and the National Youth Top-notch Talent Support Program in China. Jiafu Mao and Xiaoying Shi's time is supported by the US Department of Energy (DOE), Office of Science, Biological, and Environmental Research. Oak Ridge National Laboratory is managed by UT-BATTELLE for DOE under contract DE-AC05-00OR22725. The simulation of CLM was supported by the US Department of Energy (DOE), Office of Science, Biological, and Environmental Research.

References

Ainsworth EA, Rogers A (2007) The response of photosynthesis and stomatal conductance to rising [CO_2]: mechanisms and environmental interactions. *Plant, Cell & Environment*, **30**, 258–270.

Bai Y, Wu J, Xing Q, Pan Q, Huang J, Yang D, Han X (2008) Primary production and rain use efficiency across a precipitation gradient on the Mongolia Plateau. *Ecology*, **89**, 2140–2153.

Baldocchi DD, Verma SB, Anderson DE (1987) Canopy photosynthesis and water-use efficiency in a deciduous forest. *Journal of Applied Ecology*, **24**, 251–260.

Ball JT, Woodrow IE, Berry JA (1987) A model predicting stomatal conductance and its contribution to the control of photosynthesis under different environmental conditions. *Progress in Photosynthesis Research*, **4**, 221–224.

Beer C, Ciais P, Reichstein M *et al.* (2009) Temporal and among-site variability of inherent water use efficiency at the ecosystem level. *Global Biogeochemical Cycles*, **23**, GB2018.

Bell JE, Weng E, Luo Y (2010) Ecohydrological responses to multifactor global change in a tallgrass prairie: a modeling analysis. *Journal of Geophysical Research*, **115**, G04042.

Berry JA, Beerling DJ, Franks PJ (2010) Stomata: key players in the earth system, past and present. *Current Opinion in Plant Biology*, **13**, 233–240.

Betts RA, Cox PM, Lee SE, Woodward FI (1997) Contrasting physiological and structural vegetation feedbacks in climate change simulations. *Nature*, **387**, 796–799.

Betts RA, Cox PM, Woodward FI (2000) Simulated responses of potential vegetation to doubled-CO_2 climate change and feedbacks on near-surface temperature. *Global Ecology and Biogeography*, **9**, 171–180.

Betts RA, Boucher O, Collin M *et al.* (2007) Projected increase in continental runoff due to plant responses to increasing carbon dioxide. *Nature*, **448**, 1037–1041.

Cao L, Bala G, Caldeira K, Nemani R, Ban-Weiss G (2010) Importance of carbon dioxide physiological forcing to future climate change. *Proceedings of the National Academy of Sciences of the United States of America*, **107**, 9513–9518.

Chapin FS III, Matson PA, Vitousek P (2011) *Principles of Terrestrial Ecosystem Ecology*. Springer, New York.

Cramer W, Bondeau A, Woodward FI *et al.* (2001) Global response of terrestrial ecosystem structure and function to CO_2 and climate change: results from six dynamic global vegetation models. *Global Change Biology*, **7**, 357–373.

Cramer W, Bondeau A, Schaphoff S, Lucht W, Smith B, Sitch S (2004) Tropical forests and the global carbon cycle: impacts of atmospheric carbon dioxide, climate change and rate of deforestation. *Philosophical Transactions of the Royal Society of London. Series B: Biological Sciences*, **359**, 331–343.

De Boeck GJ, Lemmens CMHM, Bossuyt H *et al.* (2006) How do climate warming and plant species richness affect water use in experimental grasslands. *Plant and Soil*, **288**, 249–261.

De Kauwe M, Medlyn BE, Zaehle S *et al.* (2013) Forest water use and water use efficiency at elevated CO_2: a model-data intercomparison at two contrasting temperate forest FACE sites. *Global Change Biology*, **19**, 1759–1779.

Delucia E, Heckathorn S (1989) The effect of soil drought on water-use efficiency in a contrasting Great Basin desert and Sierran montane species. *Plant, Cell & Environment*, **12**, 935–940.

Dordas CA, Sioulas C (2008) Safflower yield, chlorophyll content, photosynthesis, and water use efficiency response to nitrogen fertilization under rainfed conditions. *Industrial Crops and Products*, **27**, 75–85.

Drake BG, Gonzàlez-Meler MA (1997) More efficient plants: a consequence of rising atmospheric CO_2. *Plant Physiology and Plant Molecular Biology*, **48**, 609–639.

Felzer BS, Cronin TW, Melillo JM, Kicklighter DW, Schlosser CA (2009) Importance of carbon-nitrogen interactions and ozone on ecosystem hydrology during the 21st century. *Journal of Geophysical Research*, **114**, G01020.

Feng X (1999) Trends in intrinsic water-use efficiency of natural trees for the past 100–200 years: a response to atmospheric CO_2 concentration. *Geochimica et Cosmochimica Acta*, **63**, 1891–1903.

Field CB, Jackson RB, Mooney HA (1995) Stomatal responses to increased CO_2: implications from the plant to the global scale. *Plant, Cell & Environment*, **18**, 1214–1225.

Flanagan LB, Syed KH (2011) Stimulation of both photosynthesis and respiration in response to warmer and drier conditions in a boreal peatland ecosystem. *Global Change Biology*, **17**, 2271–2287.

Gagen M, Finsinger W, Wagner-Cremer F *et al.* (2011) Evidence of changing intrinsic water-use efficiency under rising atmospheric CO_2 concentrations in Boreal Fennoscandia from subfossil leaves and tree ring δ^{13}C ratios. *Global Change Biology*, **17**, 1064–1072.

Gao G, Chen D, Xu CY, Simelton E (2007) Trend of estimated actual evapotranspiration over China during 1960-2002. *Journal of Geophysical Research*, **112**, D11120.

Gates DM (1964) Leaf temperature and transpiration. *Agronomy Journal*, **56**, 273–277.

Gerten D, Hoff H, Bondeau A, Lucht W, Smith P, Zaehle S (2005) Contemporary 'green' water flows: simulations with a dynamic global vegetation and water balance model. *Physics and Chemistry of the Earth*, **30**, 334–338.

Gitelson AA, Viña A, Masek JG, Verma SB, Suyker AE (2008) Synoptic monitoring of gross primary productivity of maize using Landsat data. *Geoscience and Remote Sensing Letters*, **5**, 133–137.

Golubev VS, Lawrinore JH, Groisman PY *et al.* (2001) Evaporation changes over the contiguous United States and the former USSR: a reassessment. *Geophysical Research Letters*, **28**, 2665–2668.

Granath G, Strengbom J, Breeuwer A, Heijmans MM, Berendse F, Rydin H (2009) Photosynthetic performance in Sphagnum transplanted along a latitudinal nitrogen deposition gradient. *Oecologia*, **159**, 705–715.

Gunderson CA, Richard LN, Wullschleger SD (2000) Acclimation of photosynthesis and respiration to simulated climatic warming in northern and southern populations of *Acer saccharum*: laboratory and field evidence. *Tree Physiology*, **20**, 87–96.

Gunderson CA, Edwards NT, Walker AV, O'hara KH, Campion CM, Hanson PJ (2012) Forest phenology and a warmer climate-growing season extension in relation to climatic provenance. *Global Change Biology*, **18**, 2008–2025.

Harris I, Jones P, Osborn T, Lister D (2014) Updated high-resolution grids of monthly climatic observations – the CRU TS3.10 Dataset. *Journal of Climatology*, **34**, 623–642.

Haverd V, Cuntz M, Griffith D, Keitel C, Tadros C, Twining J (2011) Measured deuterium in water vapour concentration does not improve the constraint on the partitioning of evapotranspiration in a tall forest canopy, as estimated using a soil vegetation atmosphere transfer model. *Agricultural and Forest Meteorology*, **151**, 645–654.

Hietz P, Wanek W, Dünisch O (2005) Long-term trends in cellulose δ^{13} C and water-use efficiency of tropical *Cedrela* and *Swietenia* from Brazil. *Tree Physiology*, **25**, 745–752.

Hobbins MT, Ramirez JA, Brown TC (2004) Trends in pan evaporation and actual evapotranspiration across the conterminous U.S.: paradoxical or complementary. *Geophysical Research Letters*, **31**, L13503.

Hovenden MJ, Newton PCD, Wills KE (2014) Seasonal not annual rainfall determines grassland biomass response to carbon dioxide. *Nature*, **511**, 583–586.

Hu Z, Yu G, Fu Y *et al.* (2008) Effects of vegetation control on ecosystem water use efficiency within and among four grassland ecosystems in China. *Global Change Biology*, **14**, 1609–1619.

Hungate BA, Reichstein M, Dijkstra P *et al.* (2002) Evapotranspiration and soil water content in a scrub-oak woodland under carbon dioxide enrichment. *Global Change Biology*, **8**, 289–298.

IPCC (2013) *Climate Change 2013: The Physical Science Basis. Contribution of Working Group I to the Fifth Assessment Report of the Intergovernmental Panel on Climate Change*. Cambridge University Press, Cambridge, UK.

Ito A, Inatomi M (2012) Water-use efficiency of the terrestrial biosphere: a model analysis focusing on interactions between the global carbon and water cycles. *Journal of Hydrometeorology*, **13**, 681–694.

Jasechko S, Sharp ZD, Gibson JJ, Birks SJ, Yi Y, Fawcett PJ (2013) Terrestrial water fluxes dominated by transpiration. *Nature*, **496**, 347–350.

Jennings K (2013) *Response of Tree Growth and Water Use Efficiency to Climate and Nitrogen Deposition in a Temperate Deciduous Forest in the Northeastern US*. University of New Hampshire, Ann Arbor.

Jung M, Reichstein M, Bondeau A (2009) Towards global empirical upscaling of FLUXNET eddy covariance observations: validation of a model tree ensemble approach using a biosphere model. *Biogeosciences*, **6**, 2001–2013.

Jung M, Reichsein M, Ciais P *et al.* (2010) Recent decline in the global land evapotranspiration trend due to limited moisture supply. *Nature*, **467**, 951–954.

Jung M, Reichstein M, Margolis HA *et al.* (2011) Global patterns of land-atmosphere fluxes of carbon dioxide, latent heat, and sensible heat derived from eddy covariance, satellite, and meteorological observations. *Journal of Geophysical Research*, **116**, G00J07.

Katul G, Manzoni S, Palmroth S, Oren R (2009) A stomatal optimization theory to describe the effects of atmospheric CO_2 on leaf photosynthesis and transpiration. *Annals of Botany*, **105**, 431–442.

Keenan TF, Hollinger DY, Bohrer G, Dragoni D, Munger JW, Schmid HP, Richardson AD (2013) Increase in forest water-use efficiency as atmospheric carbon dioxide concentrations rise. *Nature*, **499**, 324–327.

Kergoat L, Lafont S, Douville H, Berthelot B, Dedieu G, Planton S, Royer JF (2002) Impact of doubled CO_2 on global-scale leaf area index and evapotranspiration: conflicting stomatal conductance and LAI responses. *Journal of Geophysical Research*, **107**, 4808.

Knapp AK, Smith MD (2001) Variation among biomes in temporal dynamics of aboveground primary production. *Science*, **291**, 481–484.

Körner C, Basler D (2010) Phenology under global warming. *Science*, **327**, 1461–1462.

Lasch P, Lindner M, Erhard M, Suckow F, Wenzel A (2002) Regional impact assessment on forest structure and functions under climate change-the Brandenburg case study. *Forest Ecology and Management*, **162**, 73–86.

Leipprand A, Gerten D (2006) Global effects of doubled atmospheric CO_2 content on evapotranspiration, soil moisture and runoff under potential natural vegetation. *Hydrological Sciences Journal*, **51**, 171–185.

Linderson M-L, Mikkelsen TN, Ibrom A, Lindroth A, Ro-Poulsen H, Pilegaard K (2012) Up-scaling of water use efficiency from leaf to canopy as based on leaf gas exchange relationships and the modeled in-canopy light distribution. *Agricultural and Forest Meteorology*, **152**, 201–211.

Litton CM, Raich JW, Ryan MG (2007) Carbon allocation in forest ecosystems. *Global Change Biology*, **13**, 2089–2109.

Liu B, Xu M, Henderson M, Gong W (2004) A spatial analysis of pan evaporation trends in China, 1955–2000. *Journal Of Geophysical Research*, **109**, D15102.

Liu X, Zhang Y, Han W *et al.* (2013) Enhanced nitrogen deposition over China. *Nature*, **494**, 459–462.

Livingston N, Guy R, Sun Z, Ethier G (1999) The effects of nitrogen stress on the stable carbon isotope composition, productivity and water use efficiency of white spruce (*Picea glauca* (Moench) Voss) seedlings. *Plant, Cell & Environment*, **22**, 281–289.

Long SP, Ainsworth EA, Rogers A, Ort DR (2004) Rising atmospheric carbon dioxide: plants FACE the future. *Annual Review of Plant Biology*, **55**, 591–628.

Mao J, Shi X, Thornton PE, Hoffman FM, Zhu Z, Myneni RB (2013) Global latitudinal-asymmetric vegetation growth trends and their driving mechanisms: 1982–2009. *Remote Sensing*, **5**, 1484–1497.

Mazzarino M, Oliva L, Buffa E, Nuñez A, Nunez G (1991) Nitrogen mineralization and soil fertility in the dry Chaco ecosystem (Argentina). *Soil Science Society of America Journal*, **55**, 515–522.

Medlyn BE, Barton CVM, Broadmead MSJ *et al.* (2001) Stomatal conductance of forest species after long-term exposure to elevated CO_2 concentration: a synthesis. *New Phytologist*, **149**, 247–264.

Mitchell CE, Reich PB, Tilman D, Groth JV (2003) Effects of elevated CO_2, nitrogen deposition, and decreased species diversity on foliar fungal plant disease. *Global Change Biology*, **9**, 438–451.

Morison JIL (1985) Sensitivity of stomata and water use efficiency to high CO_2. *Plant, Cell & Environment*, **8**, 467–474.

Nemani RR, Keeling CD, Hashimoto H *et al.* (2003) Climate-driven increases in global terrestrial net primary production from 1982 to 1999. *Science*, **300**, 1560–1563.

Niu S, Xing X, Zhang Z *et al.* (2011) Water-use efficiency in response to climate change: from leaf to ecosystem in a temperate steppe. *Global Change Biology*, **17**, 1073–1082.

Nock CA, Baker PJ, Wanek W, Leis A, Grabner M, Bunyavejchewin S, Hietz P (2011) Long-term increases in intrinsic water-use efficiency do not lead to increased stem growth in a tropical monsoon forest in western Thailand. *Global Change Biology*, **17**, 1049–1063.

Norby RJ, Zak DR (2011) Ecological lessons from Free-Air CO_2 Enrichment (FACE) Experiments. *Annual Review of Ecology, Evolution, and Systematics*, **42**, 181–203.

Norby RJ, Warren JM, Iversen CM, Medlyn BE, McMurtrie RE (2010) CO_2 enhancement of forest productivity constrained by limited nitrogen availability. *Proceedings of the National Academy of Sciences of the United States of America*, **107**, 19368–19373.

Peng S, Piao S, Ciais P *et al.* (2013) Asymmetric effects of daytime and night-time warming on Northern Hemisphere vegetation. *Nature*, **501**, 88–92.

Peñuelas J, Canadell JG, Ogaya R (2011) Increased water use efficiency during the 20th century did not translate into enhance tree growth. *Global Ecology and Biogeography*, **20**, 597–608.

Piao S, Friedlingstein P, Ciais P, de Noblet-Ducoudré N, Labat D, Zaehle S (2007) Changes in climate and land use have a larger direct impact than rising CO_2 on global river runoff trends. *Proceedings of the National Academy of Sciences of the United States of America*, **104**, 15242–15247.

Pieruschka R, Huber G, Berry JA (2010) Control of transpiration by radiation. *Proceedings of the National Academy of Sciences of the United States of America*, **107**, 13372–13377.

Ponton S, Flanagan LB, Alstad KP *et al.* (2006) Comparison of ecosystem water-use efficiency among Douglas-fir forest, aspen forest and grassland using eddy covariance and carbon isotope techniques. *Global Change Biology*, **12**, 294–310.

Rayner DP (2007) Wind run changes: the dominant factor affecting pan evaporation trends in Australia. *Journal of Climate*, **20**, 3379–3394.

Roderick ML, Farquhar GD (2002) The cause of decreased pan evaporation over the past 50 years. *Science*, **298**, 1410–1411.

Roderick ML, Rotstayn LD, Farquhar GD, Hobbins MT (2007) On the attribution of changing pan evaporation. *Geophysical Research Letters*, **34**, L17403.

Roderick ML, Hobbins MT, Farquhar GD (2009) Pan evaporation trends and the terrestrial water balance. II. Energy balance and interpretation. *Geography Compass*, **3**, 761–780.

Sen PK (1968) Estimates of the regression coefficient based on Kendall's tau. *Journal of the American Statistical Association*, **63**, 1379–1389.

Serrat-Capdevila A, Scott RL, Shuttleworth WJ, Valdés JB (2011) Estimating evapotranspiration under warmer climates: insights from a semi-arid riparian system. *Journal of Hydrology*, **399**, 1–11.

van der Sleen P, Groenendijk P, Vlam M et al. (2015) No growth stimulation of tropical trees by 150 years of CO_2 fertilization but water-use efficiency increased. *Nature geoscience*, **8**, 24–28.

Sun F, Kuang Y, Wen D, Xu Z, Li J, Zuo W, Hou E (2010) Long-term tree growth rate, water use efficiency, and tree ring nitrogen isotope composition of *Pinus massoniana L*. in response to global climate change and local nitrogen deposition in Southern China. *Journal of Soils and Sediments*, **10**, 1453–1465.

Tang J, Bolstad PV, Ewers BE, Desai AR, Davis KJ, Carey EV (2006) Sap flux–upscaled canopy transpiration, stomatal conductance, and water use efficiency in an old growth forest in the Great Lakes region of the United States. *Journal of Geophysical Research*, **111**, G02009.

Tian H, Chen G, Liu M *et al.* (2010) Model estimates of net primary productivity, evapotranspiration, and water use efficiency in the terrestrial ecosystems of the southern United States during 1895–2007. *Forest Ecology and Management*, **259**, 1311–1327.

Tucker CJ, Slayback DA, Pinzon JE, Los SO, Myneni RB, Taylor MG (2001) Higher northern latitude normalized difference vegetation index and growing season trends from 1982 to 1999. *International Journal of Biometeorology*, **45**, 184–190.

Wang K, Dickinson RE (2012) A review of global terrestrial evapotranspiration: observation, modeling, climatology, and climatic variability. *Reviews of Geophysics*, **50**, RG2005.

Wang YP, Law RM, Pak B (2010) A global model of carbon, nitrogen and phosphorus cycles for the terrestrial biosphere. *Biogeosciences*, **7**, 2261–2282.

Wullschleger SD, Gunderson C, Hanson P, Wilson K, Norby R (2002) Sensitivity of stomatal and canopy conductance to elevated CO_2 concentration – interacting variables and perspectives of scale. *New Phytologist*, **153**, 485–496.

Yu G, Song X, Wang Q *et al.* (2008) Water-use efficiency of forest ecosystems in eastern China and its relations to climatic variables. *New Phytologist*, **177**, 927–937.

Zhang Q, Wang Y, Matear R, Pitman A, Dai Y (2014) Nitrogen and phosphorous limitations significantly reduce future allowable CO_2 emissions. *Geophysical Research Letters*, **41**, 632–637.

Zhao M, Running W (2010) Drought-induced reduction in global terrestrial net primary production from 2000 through 2009. *Science*, **329**, 940–943.

Zhao M, Heinsch FA, Nemani RR, Running SW (2005) Improvements of the MODIS terrestrial gross and net primary production global data set. *Remote Sensing of Environment*, **95**, 164–176.

Zhou L, Tucker CJ, Kaufmann RK, Slayback D, Shabanov NV, Myneni RB (2001) Variations in northern vegetation activity inferred from satellite data of vegetation index during 1981 to 1999. *Journal of Geophysical Research*, **106**, 20069–20083.

Zhu Q, Jiang H, Peng C *et al.* (2011) Evaluating the effects of future climate change and elevated CO_2 on the water use efficiency in terrestrial ecosystems of China. *Ecological Modelling*, **222**, 2414–2429.

Zhu Q, Jiang H, Peng C *et al.* (2012) Effects of future climate change, CO_2 enrichment, and vegetation structure variation on hydrological processes in China. *Global and Planetary Change*, **80–81**, 123–135.
Zhu Z, Bi J, Pan Y *et al.* (2013) Global data sets of vegetation leaf area index (LAI) 3 g and Fraction of Photosynthetically Active Radiation (FPAR) 3 g derived from Global Inventory Modeling and Mapping Studies (GIMMS) Normalized Difference Vegetation Index (NDVI3 g) for the period 1981 to 2011. *Remote Sensing*, **5**, 927–948.

Supporting Information

Additional Supporting Information may be found in the online version of this article:

Table S1. Details of process-oriented models used in this study.
Figure S1. Spatial patterns of 'CO_2'-only DGVM modeled trendof TR/LAI (the unit transpiration per unit LAI) from 1982 to 2008.
Figure S2. Spatial patterns of (a) evapotranspiration trends from 1982 to 2008; (b) transpiration trends from 1982 to 2008; (c) evaporation trends from 1982 to 2008; (d) relative change of mean LAI of the last 5 years of study period compared with mean LAI of the first 5 years of study period under DGVMs simulation S1.
Figure S3. Spatial patterns of (a) k, the ratio between the average EWUE from 1982 to 1986 and that from 2004 to 2008 estimated by MTE model, (b) k′, the theoretical ratio between the average theoretical EWUE from 1982 to 1986 and that from 2004 to 2008 if the effects of elevated CO_2 on stomatal conductance and LAI are both taken into consideration.